BOUNDARY ELEMENT METHOD APPLIED TO SOFT TISSUES ELASTOGRAPHY

Santiago, A. G.[*, **] Trintinalia, L. C.[**], Gutierrez, M. A.[*]

* – InCor - HCFMUSP, São Paulo, Brazil
** – Engenharia Elétrica - Escola Politécnica da USP, São Paulo, Brazil

email: gsantiago@usp.br

Abstract: This paper presents an application of the Boundary Element Method (BEM) as a tool for elastographic studies. In this area, one of the most used methods is the Finite Element Method (FEM), which needs a mesh over the whole domain of the image being analyzed. In the proposed study, the BEM needs only the contour of each structure present in the image, resulting into a more efficient pre-processing, smaller and better conditioned matrices and faster inverse problem analysis when compared to FEM. The proposed methodology is applied to mathematical phantoms and the results obtained are compared with FEM.

Keywords: Boundary element method, Finite element method, Elastrography, Complex variable analysis.

Introduction

Elastography is a method that can be used in any tissue system that is imaged by ultrasound and which can be subjected to a small static or dynamic compression. The compression may be applied externally or internally by any physiological phenomena, such as pulsating arteries, respiration or any other mechanical stimulus. The resulting strains are used to estimate the material properties of the tissues being analyzed. Elastography is a non invasive technique, it can be applied for example, to breast cancer detection, since tissues abnormalities are associated with changes in the mechanical properties.

One of the most used methods for displacements estimation is the cross correlation technique [1]. Some authors also present alternative methods for displacements mapping [1, 2]. A main characteristic of these approaches is that they present only a strain analysis, which can be insufficient to characterize the tissues present in the image.

Some numerical methods can be used in order to determine the mechanical properties of the tissues being imaged. Guo et. al. [3] presents a methodology for elastography using the Finite Element Method (FEM) and inverse problem analysis. Baldewsing et. al. [4] and Moraes et al. [5] also use FEM to perform their studies in elastography. The main problem with FEM is that it needs a mesh over the whole domain of the problem, leading to great coding effort to create the mesh, and for a fine grid of elements, it is time and memory consuming for generating the meshes and for simulations.

Another approach to overcome these problems is to consider the Boundary Element Method (BEM). The BEM is a numerical technique used to solve boundary value problems by discretizing only the contour of the domain. It has many practical applications in many areas of Mathematical Physics, such as Continuum Mechanics, Acoustics and Electromagnetism [6]. It uses only a mesh over the boundaries of the problem, which in the present case, can be obtained easily by manual segmentation or some reliable border detection algorithm such as Canny, instead of awkward and time consuming algorithms to create mesh grids over an image. BEM also results into smaller and better conditioned matrices when compared to FEM.

In this paper we propose a new methodology for elastography based on BEM, which includes simulations using mathematical phantoms. A comparison of the computational cost and convergence rate between BEM and FEM in to solve the same problem is also presented.

Materials and methods

The Boundary Element Method -

In order to perform the elastographic study, the BEM is applied to the equilibrium force equation, and with the constitutive and the strain-displacement relation, it results in the Boundary Integral Equation (BIE), given by Equation 1.

$$\sum_k C_{ik}(\xi)\boldsymbol{u}_k(\xi) + \sum_k \int_\Gamma T_{ik}(x,\xi)\boldsymbol{u}_k(x)d\Gamma(x) = \sum_k \int_\Gamma U_{ik}(x,\xi)\boldsymbol{t}_k(x)d\Gamma(x) \qquad i,k = 1,2 \tag{1}$$

In Equation 1, Γ is the boundary of the domain, the value of $C_{ik}(\xi)$ depends on the local geometry of Γ at ξ, $t(x)$ and $u(x)$ are the surface tractions and displacements, $T(x, \xi)$ and $U(x, \xi)$ are the fundamental solution for 2D stress and displacements; They represent the tractions and displacements in the i-th direction at x due to an unity load line in the i-th direction applied in ξ, in a plane homogeneous infinite body. Details about the derivation of these equations can be found at [4]. By dividing the surface Γ into N_{el} boundary elements, the

surface tractions and displacements can be interpolated in each element Γ_{el} using shape functions, as in Equations 2 and 3.

$$t_i(\vec{x}) = \sum N_j(\vec{x}) t_{ij} \tag{2}$$

$$u_i(\vec{x}) = \sum N_j(\vec{x}) u_{ij} \tag{3}$$

In Equations 2 and 3, j is the j-th interpolation function used to describe the variable field and t_{ij} and u_{ij} are the nodal values of tractions and displacements.

Substituting Equations 2 and 3 into Equation 1 results in the discretized form of BIE, Equation 4.

$$\sum_k C_{ik}(\xi) u_k(\xi) + \sum_k \int_\Gamma T_{ik}(x,\xi) u_k(x) d\Gamma(x) = \sum_k \int_\Gamma U_{ik}(x,\xi) t_k(x) d\Gamma(x) \qquad i,k = 1,2 \tag{4}$$

A linear system of equations relating the tractions and surface displacements is obtained by varying the source point ξ_α over the surface Γ, as in Equation 5.

$$[H]\{u\} = [G]\{t\} \tag{5}$$

For the proposed problem, constant shape function was chosen, i.e., $N(\xi) = 1$, which means that the variables (tractions and surface displacement) are considered to be constant over the element and discontinuous between two adjacent elements.

Discontinuous elements are characteristic of BEM, and they allow an efficient parallel computational treatment, since the BEM code is implemented in a General Purpose Graphics Processor Unit (GpGPU – GeForce GTX 690) using *Compute Unified Device Architecture* (CUDA) and MatLab [7]. In this case, each element sub matrix can be evaluated in a thread and there is no need for matrix assembly.

After imposing the boundary conditions of tractions and displacements into Equation 5, the resulting linear system (Eq. 6), is solved for the unknown vector {x}, which may contain both unknown tractions and displacements.

$$[A]\{x\} = \{b\} \tag{6}$$

Mathematical Phantoms – Mathematical phantoms can be used in order to simulate soft tissues for the proposed study. In this paper, a phantom with a cross section of *50x50mm* were considered, having 3 circular inclusions each one of them with a different Young's modulus but with the same Poisson ratio of $\nu = 0.495$ for all the materials considered [8] (Figure 1).

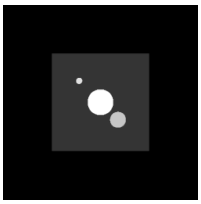

Figure 1: Mathematical phantoms with three inclusions.

For the proposed models, the Young's modulus of the background is $E_{back} = 20KPa$, and $r_1 = 1.5mm$, $r_2 = 6.5mm$ and $r_3 = 4mm$, $E_{inc1} = 25KPa$, $E_{inc2} = 600KPa$ and $E_{inc3} = 750KPa$, placed in $(x_1, y_1) = (14, 14)mm$, $(x_2, y_2) = (25, 25)mm$ and $(x_3, y_3) = (34, 34)mm$.

Nodes were placed around the contour of each structure, i.e., plaque and inclusions, and boundary element and finite element meshes were created in order to compare the results.

The finite element meshes were created using the boundary nodes and the software Gmsh [9], and linear first order finite element triangles were used as shape functions.

In order to simulate the mechanical behavior of the proposed phantoms and generate data for the elastographic study, a load of 10KPa was applied at the top of each phantom and the bottom is fixed, avoiding displacements in x and y directions, as shown in Figure (2).

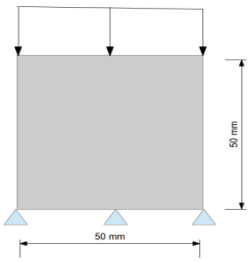

Figure 2: Boundary conditions.

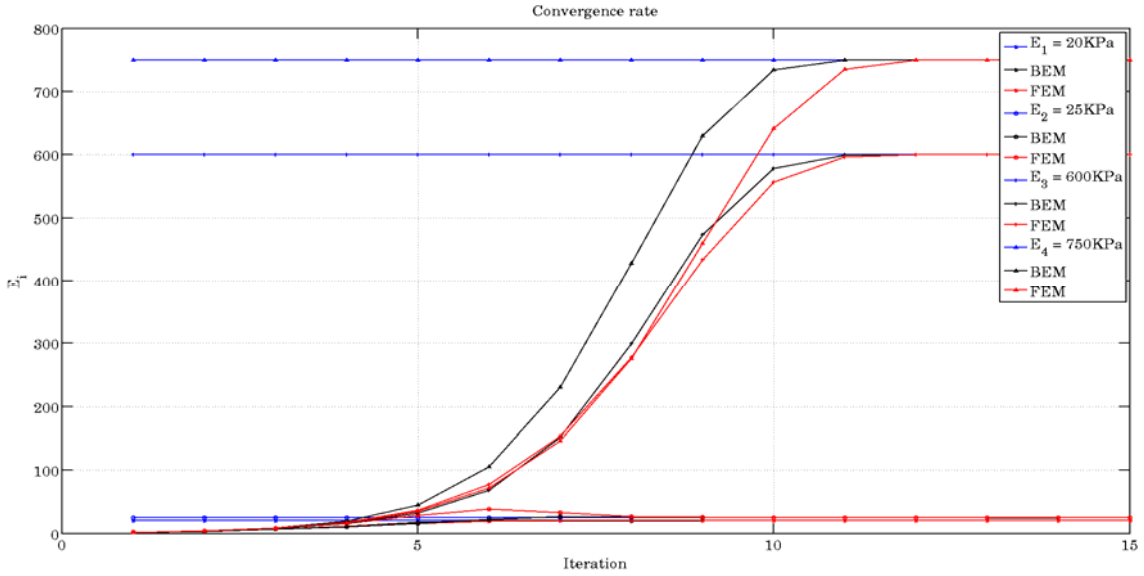

Figure 3: Convergence rate for the phantom in Figure 1.

Simulations were carried out using both BEM and FEM, also implemented in GpGPU [10].

Complex Variable Analysis and Inverse Problem – In order to evaluate the derivatives needed for the inverse analysis problem, a complex variable approach is used. It is summarized in Equation 4

$$\frac{\partial f(\beta,\vec{y})}{\partial \beta} = \frac{\Im(f(\beta + jh,\vec{y}))}{h} \qquad (4)$$

j is the complex unity and $\Im(*)$ is the imaginary component of $f(y)$ evaluated at $\beta = \beta_i + jh$.

In the proposed study, $h = 10^{-6}$ was used. The main advantage of this approach is that it results in semi analytical derivatives, which avoids round off errors [9].

The Young's modulus for each component was estimated using an iterative approach.

Equation 1 is evaluated using an initial estimative of $E_i = 1KPa$ for every Young modulus in the problem. For each interaction, the reminder is evaluated as described in [11].

Results – The proposed phantom in Figures 1 were simulated using both BEM and FEM as described in this paper. The phantom is used to simulate the behavior of soft tissues with inclusions and different values of Young's moduli for each inclusion.

The displacement fields obtained by the simulations were used as input data for the proposed methodology in order to investigate the accuracy of the inverse problem analysis. The results obtained were compared to those obtained by FEM analysis, showing a better convergence rate or at least, the same convergence rate.

The convergence for Young's moduli for the proposed phantom in Figure 1 are presented in Figure 3, considering a minimum tolerance of 10^{-6} and sixteen iterations; The displacement field used as input for the proposed methodology is presented in Figure 4.

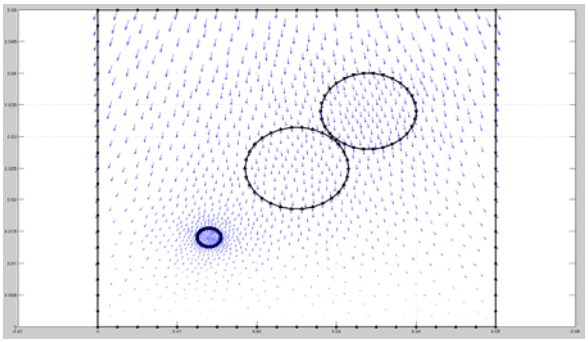

Figure 4: Displacement field for phantom of Figure 1.

Table 1 compares the computational cost considering the number of elements in BEM and FEM meshes for each phantom.

N. of Inclusions	BEM analysis (s)	N. of Boundary Elements	FEM analysis (s)	N. of Finite Elements
1	0.3493	68	1.6797	416
2	2.6059	200	32.9371	2030
3	9.5541	260	73.6151	2664

Discussion and Conclusion

Considering sixteen iterations and an error of 10^{-6}, both FEM and BEM show the same profile of convergence, but BEM tends to approach the correct value faster than FEM in some cases, as can be observed in Figure 4.

Observing the computational cost for the analysis, presented in Table 1, BEM can be 4.8 up to 12 times

faster than FEM, since it uses 6.11 up to 10.24 times fewer elements, and there is no need for matrix assembly, as stated earlier in this paper, due to the use of discontinuous elements.

The mesh generation must be considered too. Generating a boundary element mesh consists in placing nodes around the contours of every structure present in the image and connecting those points in a sequential manner, while in finite element mesh generation, complex meshing algorithms must be used.

References

[1] Liu K, Zhang P, Zhu X, Zhang Y, Bai J. A 2D strain estimator with nimeical optimization method for soft-tissue elastography. In: Elsevier, Ultrasonics (2009), p. 723 – 732.

[2] Pan X, Gao J, Tao S, Liu K, Bai J, Luo J. A Two Step Optical Flow for Strain Estimation in Elastography: Simulation and Phantom Study. In: Elsevier, Ultrasonics (2014), p. 990 – 996.

[3] Guo Z, You S, Wan X, Bicniac, N. A FEM-based direct method for material reconstruction inverse problem in soft tissue elastography. In: Elsevier, Computer and Structures (2010), p. 1459 – 1468.

[4] Baldewsing RA, de Korte CL, Schaar JA, Mastik F, van der Steen AFW. A Finite Element Model for Performing Intravascular Ultrasound Elastography of Human Artherosclerotic Coronary Arteries. Ultrasound Med. Biol. 2004; 30(6): 803-813

[5] Moraes MC, Cardoso FM, Furuie SS, Atherosclerotic Tissue Classification by Plaque Area Ratio in Ivus Images. In: XXIII Congresso Brasileiro em Engenharia Biomédica – XXIII CBEB.

[6] Gaul L, Kögl M, Wagner M. Boundary Element Methods for Engineers and Scientists: An Introductory Course with Advanced Topics, Springer 2002.

[7] Labaki J, Ferreira LOS, Mesquita E. Constant Boundary Elements on Graphics Hardware: a GPU-CPU Complementary Implementation. Journal of the Brazilian Society of Mechanical Sciences and Engineering, v. XXXIII, p. 475-482, 2011.

[8] Akyildiz AC, Speelman L, Gijsen FJH. Mechanical Properties of Human Atherosclerotic Intima Tissue. Elsevier, Journal of Biomechanics, Vol. 47 (4), March 2014, p. 773 – 783.

[9] Geuzaine C, Remacle JF. Gmsh: a three-dimensional finite element mesh generator with built-in pre and post-processing facilities. International Journal for Numerical Methods in Engineering, 79(11), 2009, p. 1309-1331

[10] Cecka C, Lew AJ, Darve E. Assembly of Finite Element Methods on Graphics Processors. Int. J. Numer. Meth. Engng, 2000.

[11] Gao XW, He MC. A New Inverse Analysis Approach for Multi-Region Heat Conduction BEM Using Complex-Variable-Differentiation Method. Elsevier, Eng. Analysis with Boundary Elements 29, 2005, p. 788 – 795.